Journal of Hazardous Materials 262 (2013) 83–90

Contents lists available at ScienceDirect

Journal of Hazardous Materials

journal homepage: www.elsevier.com/locate/jhazmat

Novel hydrophobic PDVB/R-SiO_2 for adsorption of volatile organic compounds from highly humid gas stream

Han-feng Lu*, Jie-jing Cao, Ying Zhou, De-li Zhan, Yin-fei Chen

College of Chemical Engineering and Materials Science, Research Institute of Catalytic Reaction Engineering, Zhejiang University of Technology, Hangzhou 310014, China

HIGHLIGHTS

- Novel organic–inorganic adsorbent PDVB/R-SiO_2 was successfully prepared.
- The amount of toluene adsorbed on PDVB/R-SiO_2 is 12 times that on SiO_2.
- A highly humid environment exhibits no effect on the dynamic adsorption of PDVB/R-SiO_2.

GRAPHICAL ABSTRACT

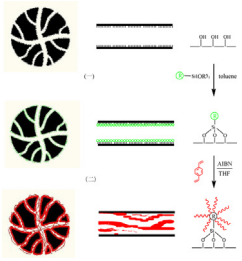

ARTICLE INFO

Article history:
Received 19 May 2013
Received in revised form 4 August 2013
Accepted 13 August 2013
Available online 21 August 2013

Keywords:
SiO_2
Polydivinylbenzene
Organic–inorganic
Adsorbent
Volatile organic compounds
Hydrophobicity

ABSTRACT

A novel organic–inorganic hydrophobic polydivinylbenzene–silica adsorbent (PDVB/R-SiO_2) was successfully prepared by introducing a specific amount of divinylbenzene and solvent (i.e., tetrahydrofuran) to SiO_2 pores and initiating polymerization under solvothermal conditions. New smaller structures and surface areas were formed in the SiO_2 pores. The PDVB/R-SiO_2-0.5 samples exhibited a bimodal pore size distribution with both SiO_2 micropores/mesopores (0.5–2.0 nm) and mesopores (2.0–5.0 nm). The surface areas increased from 116 m^2/g (SiO_2) to 246 m^2/g. The breakthrough curves of toluene adsorption indicated that the amount adsorbed on PDVB/R-SiO_2-0.5 was 12 times higher than that on SiO_2. The highly humid environment exhibited no effect on adsorption because the surface of PDVB was functionalized. The adsorbed toluene was easily desorbed in hot N_2 stream at 100 °C. After 10 adsorption–desorption cycles, PDVB/R-SiO_2-0.5 continued exhibiting excellent adsorption, indicating superior structural and regeneration abilities.

1. Introduction

Emissions of volatile organic compounds (VOCs) in industrial processes need to be addressed immediately. Adsorption can effectively reduce VOCs for a flexible system with low energy and operating cost, as well as recover high-value VOCs [1]. Various nanoporous materials have been developed as adsorbents, such as activated carbon, zeolites, and mesoporous materials. Activated carbon is preferred among these materials because of its large surface area, high porosity, and sustainability [2,3]. However, the development of activated carbon has been limited by several disadvantages, such as increased fire risk, pore clogging, hygroscopicity, and loss of regenerative ability [4–8]. As an alternative, zeolite can adsorb several small organic substances [9–12]. However, zeolite cannot adsorb large organic molecules in high-humidity gas streams because zeolite lacks mesopores and a hydrophobic surface [13,14]. Commercially available mesoporous molecular sieves, such as SBA-15 and MCM-41, can also be used as adsorbents [15–17]. However, these molecular sieves fail to exhibit high adsorptive capacity and stability at low pressure [18–20]. Moreover, fabrication of these molecular sieves requires costly raw materials and involves complex synthesis, thus impeding

* Corresponding author. Tel.: +86 571 88320767; fax: +86 571 88320767.
E-mail addresses: luhf@zjut.edu.cn, lu.hanfeng@gmail.com (H.-f. Lu).

0304-3894/$ – see front matter © 2013 Elsevier B.V. All rights reserved.
http://dx.doi.org/10.1016/j.jhazmat.2013.08.033

the large-scale application of these sieves. Therefore, a novel and efficient material with high adsorption capacity, hydrophobicity, and stable performance needs to be developed.

Silica gel (SiO_2) exhibits potential as a superior alternative to activated carbon and molecular sieves because of its controllable pore structure, large surface area, structural stability, and excellent regeneration ability [12,21]. Silica gel acts as an excellent desiccant in rotary dehumidifiers, which remove water vapor from workshops [22,23]. However, the surface of silica gel is rich in hydroxyl groups, which leads to strongly hydrophilic and relatively low adsorption capacity of organic molecules in highly humid environments. The pore size of silica gel is generally greater than 4 nm, which facilitates the diffusion of organic molecules and consequently reduces the adsorption capacity of these molecules in low-concentration organic waste gas. With the efficient adsorption of VOCs considered, the hydrophobicity of groups on the silica surface and the porosity of silica gel must be controlled.

Polydivinylbenzene (PDVB) resin prepared by the solvothermal route is a superhydrophobic nanoporous material with large surface area and pore volume, as well as excellent adsorptive property for organic molecules relative to activated carbon [24,25]. Therefore, if divinylbenzene (DVB) can be introduced to the macropores of silica gel and polymerized in these pores by the solvothermal method, the hydrophobicity of the silica gel surface would increase, and the pore size of the silica gel would be reduced.

This study aims to (1) design a method of introducing DVB to the macropores of silica gel and create new micropores/mesopores; (2) investigate the effect of the amount of PDVB on the pore structure, surface area, hydrophobicity, and VOC adsorption capacity of silica gel; and (3) examine VOC adsorption and desorption on organic–inorganic PDVB–silica adsorbents.

2. Experimental

2.1. Preparation of adsorbents

The preparation of PDVB/SiO_2 composite adsorbents is schematically shown in Fig. 1. Silica gel was silanized by grafting to provide it with hydrophobic groups. Silanizaiton pretreatment was conducted to transform the surface properties of silica gel from being hydrophilic to hydrophobic. Non-polar divinylbenzene (DVB) can then be introduced into the pores of silica gel by dispersion, thereby preventing polymerization on the outer surface of the silica gel. Up to 1.0 g of commercial silica gel (SiO_2, Qingdao Guijiao Meigao, China), 50 mL of toluene, and 10 mL of KH-570 [γ-(methacryloxypropyl)trimethoxy silane] were mixed and refluxed at 85 °C for 10 h. The white vinyl-functionalized SiO_2 was repeatedly washed with ethanol and dried at room temperature. The sample was labeled as R-SiO_2.

DVB was dissolved in varying amounts of tetrahydrofuran (THF) solvent at ratios of [DVB/THF (wt)] 1:0.5, 1:1, 1:2, and 1:3. Azobisisobutyronitrile (0.01 g) was subsequently added to these solutions. After stirring for 30 min at 0 °C, the 1.0 mL solution thoroughly mixed with 1 g of R-SiO_2. The samples were placed in an autoclave and treated at 110 °C for 30 h. The system was cooled to room temperature, and samples were obtained after slow evaporation of the THF. The synthesized materials were designated as PDVB/R-SiO_2-*x*, where *x* is the DVB/THF ratio (i.e., 2.00, 1.00, 0.50, and 0.33).

2.2. Characterization

The physical characteristics of the adsorbents, including their specific surface area, pore volume distribution, and pore diameter, were measured by N_2 (g) adsorption in an ASAP 2020 micropore analyzer at 77 K in liquid N_2. Surface area was calculated according to the Brunauer–Emmett–Teller method by using adsorption data acquired at a relative pressure (P/P_0) ranging from 0.05 to 0.25. The total pore volume was estimated based on the amount adsorbed at a relative pressure of about 0.99. Pore size distribution curves were derived from the analysis of the desorption branch of the isotherm according to the Barrett–Joyner–Halenda algorithm. Fourier transform infrared (FTIR) spectra were obtained by the KBr method, recorded on a Bruker Vector-70, and scanned from 4000 cm^{-1} to 500 cm^{-1}. The thermogravimetry (TG) and the derivative thermogravity (DTG) results of the samples were analyzed with a TG/DTG analyzer (NETZSCH, STA 409PC). The heating rate was set at 10 K/min from 50 °C to 850 °C under an N_2 flow of 50 mL/min. The water contact angles of the samples were measured with a theta optical tensiometer (KSV Instruments) and electro-optics with a closed-circuit television camera connected to a computer (Attension Theta software). A droplet of distilled water (3 μL) was deposited on the surface of the samples. The water contact angle of each sample was measured three times, and the average value was recorded.

2.3. Adsorption performance test

Toluene was used as a model VOC. Gaseous toluene was generated by bubbling liquid toluene at 0 °C with nitrogen gas flow. The flow volume was regulated by a mass flow controller. The generated gaseous toluene was transferred to a buffer by N_2 steam and then diluted with N_2 at the required concentration. The gaseous toluene was then passed directly through a sample column at 40 °C. The column (8 mm in diameter, 13 mm in height) was packed with the adsorbent of about 0.5 g. The inlet and the outlet toluene concentrations were monitored online by an HP-Agilent 7890 gas chromatograph equipped with a flame ionization detector. The inlet toluene concentration was controlled at 1000 mg/m^3. Adsorption capacity was calculated according to Eq. (1):

$$q = \frac{F \times C_0 \times 10^{-9}}{W}\left[t_s \int_0^{t_s} \frac{C_i}{C_0} dt\right] \quad (1)$$

where q is the dynamic adsorption capacity (mg/g), t_s is the time to reach adsorption equilibrium (min), F is the flow volume of the carrier gas (N_2) (500 mL/min), W is the weight of the adsorbent (g), C_0 is the inlet concentration of the adsorbed gas (mg/m^3), and C_i is the outlet concentration of the adsorbed gas (mg/m^3).

The influence of water vapor was also measured according to the above procedure. The N_2 steam was humidified directly by using an electronic humidifier and then passed through a sample column. Humidity levels at the inlet and the outlet of the column were monitored using a humidity sensor.

2.4. Regeneration ability

After the saturated adsorption of toluene, the samples were regenerated by a hot N_2 stream of 20 mL/min at 100 °C for 60 min. The samples were reused to measure adsorption ability. The same procedure was repeated 10 times during subsequent recycling.

3. Results and discussion

3.1. Physicochemical and texture characteristics

The amount, thermal stability, and distribution of PDVB in the pores and on the surface of the silica gel were investigated by thermal analysis. The weight loss (TG) and differential weight analysis (DTG) results of SiO_2, R-SiO_2, and PDVB/R-SiO_2 are presented in Fig. 2. The TG profile of SiO_2 shows that only one stage of weight

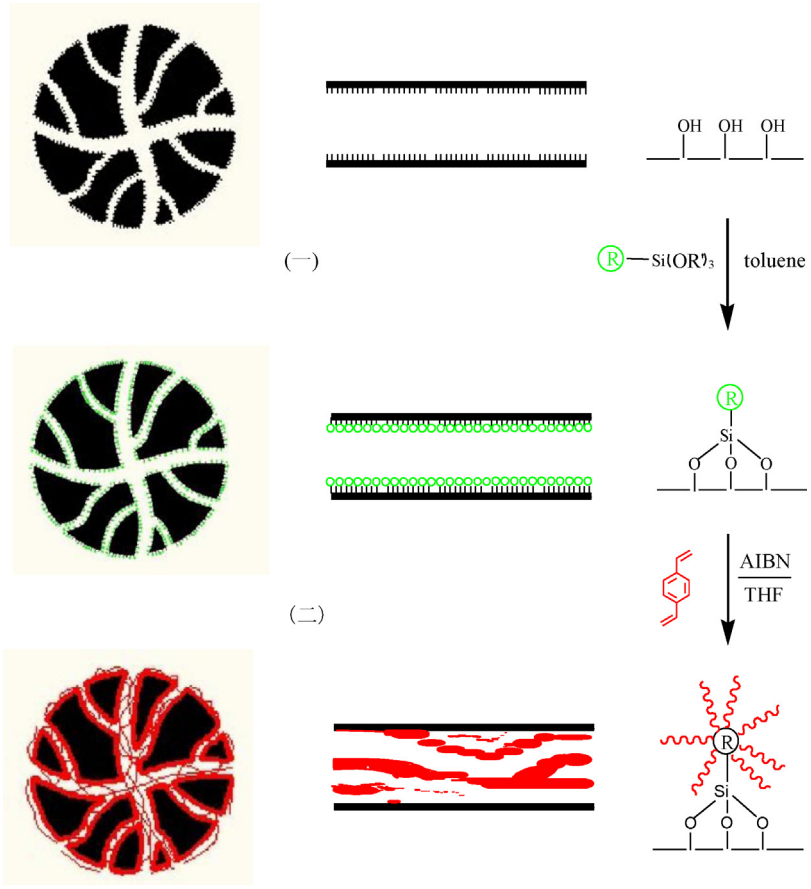

Fig. 1. Schematic model for preparing the organic–inorganic composite adsorbent of PDVB/R-SiO_2.

loss before 200 °C is attributed to the loss of adsorbed water. After silane was grafted onto SiO_2, the R-SiO_2 sample exhibited an additional weight loss of 5 wt% at temperatures ranging from 260 °C to 450 °C, which corresponded to silane decomposition. This finding suggests that silane was successfully grafted onto the surface of the silica gel. The TG curves of the PDVB/R-SiO_2 samples revealed two stages of weight loss – one ranging from 250 °C to 450 °C and the other from 450 °C to 700 °C – and a total weight loss of more than 20 wt%. These results indicate the thermal decomposition of the PDVB resin. However, Fig. 2 and [24] show that the temperature of pure PDVB decomposition ranged from 250 °C to 500 °C. Thus, the weight loss when the temperature ranged from 250 °C to 500 °C can be attributed to the decomposition of PDVB on the external surface of the SiO_2, and SiO_2 exerts no effect on the thermal decomposition of PDVB. However, the decomposition temperature of PDVB/R-SiO_2 ranges from 250 °C to 700 °C, which is obviously wider than that of pure PDVB. These results suggest that the decomposition of PDVB occurs at higher temperatures because part of PDVB entered into the pores of SiO_2. The increase in decomposition temperature may be attributed to the following. (1) Heat transfer effect. During the heating process, heat transfer from the outer to the inner surface of SiO_2 is very slow because of the low thermal conductivity of SiO_2 [0.35 W/(m K)]. Therefore, the actual temperature in the pores is consistently lower than the temperature recorded by TG; (2) diffusion effect. The diffusion of the products of the decomposition of PDVB is impeded by the diffusion resistance of the pores. Therefore, the decomposition of PDVB in the pores is slower than that on the external surface. As shown in Fig. 2, decomposition occurs at a higher temperature as the DVB/THF ratio increases. This result suggests that the DVB monomer was successfully introduced to the pores of the silica gel. When the external surfaces of the silica gel adsorbed DVB to saturation, the excess DVB and solvent quickly penetrated the pores.

The FTIR spectra of SiO_2, R-SiO_2, and PDVB/R-SiO_2 are compared in Fig. 3. The vibration bands around 3430 cm^{-1} and a shoulder around 1635 cm^{-1} indicate the presence of molecular water and Si—OH. All sample spectra exhibited a wide absorption band in the range of 900–1300 cm^{-1}; this band can be attributed to the Si—O—Si stretching vibration. However, compared with that of pure SiO_2, the adsorption band intensity of Si—OH of the R-SiO_2 and PDVB/R-SiO_2 samples was significantly reduced, and a new adsorption band centered on 750 and 2930 cm^{-1} appeared. This new band is attributed to benzene and C—H vibration, indicating that the silane (KH-570) and PDVB grafted and loaded onto the surface of the silica gel formed an organic–inorganic composite material.

3.1.1. *Surface area and pore volume distribution*

The surface areas and pore volumes of the samples are listed in Table 1. SiO_2 exhibited a relatively small surface area of 119 m^2/g and a large pore size. After silane was grafted, it occupied part of the silica gel surface area, further reducing the R-SiO_2 surface area. However, the surface area of the samples expanded when PDVB was introduced to the pores of the silica gel. PDVB/R-SiO_2-0.5 exhibited the largest surface area of 246 m^2/g, which is twice that of pure silica gel. The increase in surface areas indicates that the PDVB resin filled the pores of SiO_2 and created more micropores in the mesopore structure of the silica gel. Excess PDVB introduced to the SiO_2 pores inhibited the creation of new pores and reduction of the surface area because it blocked the pores.

The nitrogen adsorption/desorption isotherms and pore size distribution of the samples are shown in Fig. 4(A) and (B). The adsorption isotherms were of type IV (International Union of Pure

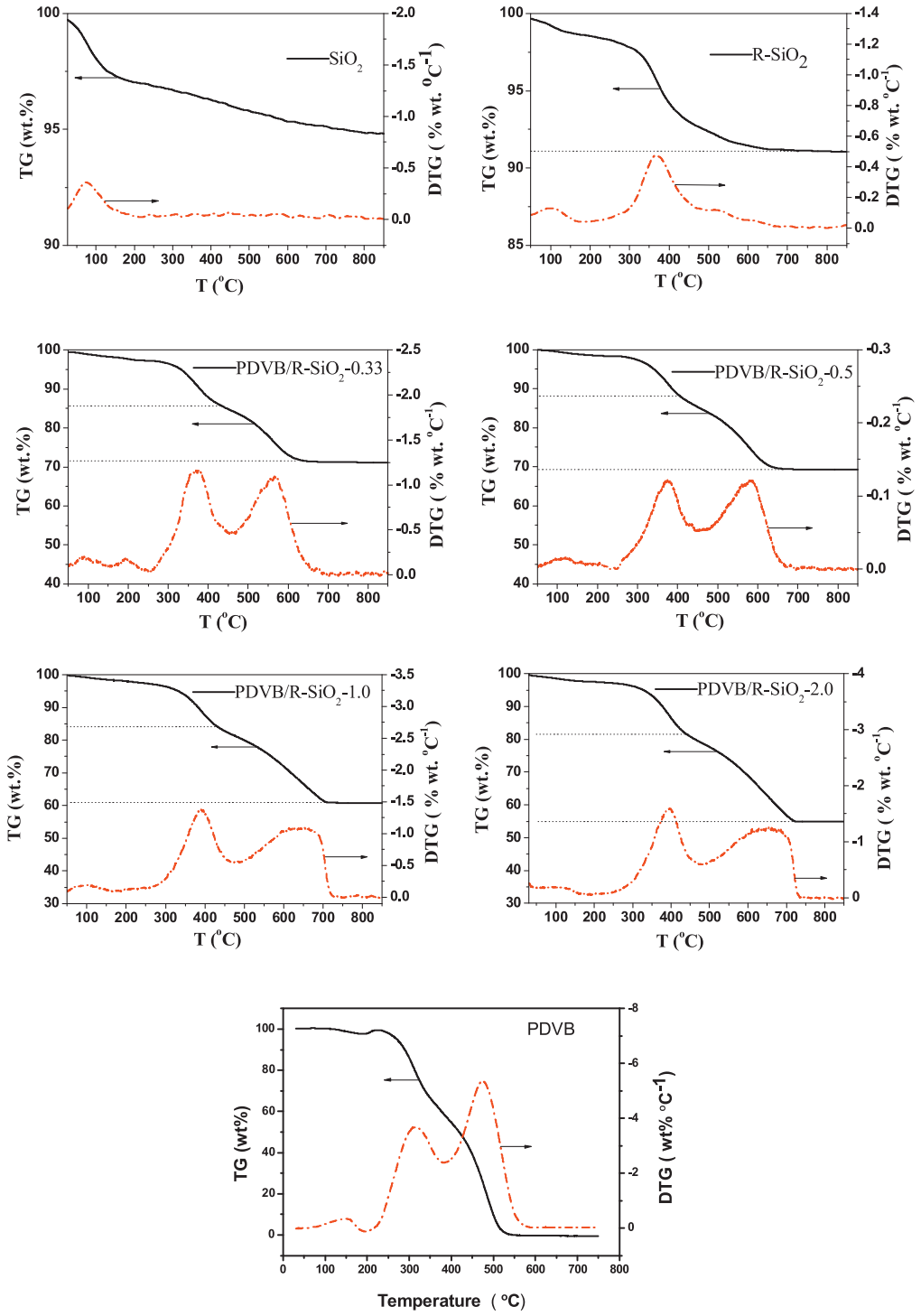

Fig. 2. TG and DTG curves for SiO_2, R-SiO_2, PDVB/R-SiO_2 and PDVB samples.

Table 1
Textural properties of SiO_2, R-SiO_2 and PDVB/R-SiO_2 samples.

Sample	DVB/THF in solvent	BET (m^2/g)	Pore volume (m^3/g)	Average pore size (nm)	Micropore volume (cm^3/g)	Micropore area (m^2/g)	PDVB loading%[a]
SiO_2	–	119.0	0.252	30.33	0.005	4.222	–
R-SiO_2	–	100.7	0.248	26.65	0.007	5.236	–
PDVB/R-SiO_2-0.33	1/3	133.7	0.167	20.01	0.012	20.92	24
PDVB/R-SiO_2-0.5	1/2	246.5	0.272	10.09	0.064	65.27	27
PDVB/R-SiO_2-1.0	1/1	27.61	0.065	36.48	0.002	3.932	34
PDVB/R-SiO_2-2.0	1/0.5	15.65	0.037	40.21	–	–	41

[a] Data was calculated from TG curves.

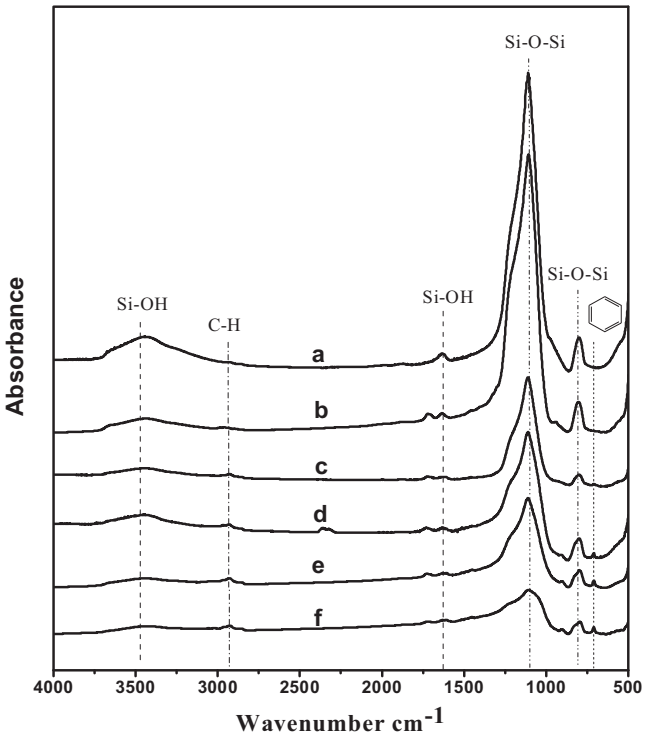

Fig. 3. FT-IR spectra of patterns of samples. (a) SiO_2; (b) R-SiO_2; (c) PDVB/R-SiO_2-0.33; (d) PDVB/R-SiO_2-0.5; (e) PDVB/R-SiO_2-1.0; (f) PDVB/R-SiO_2-2.0.

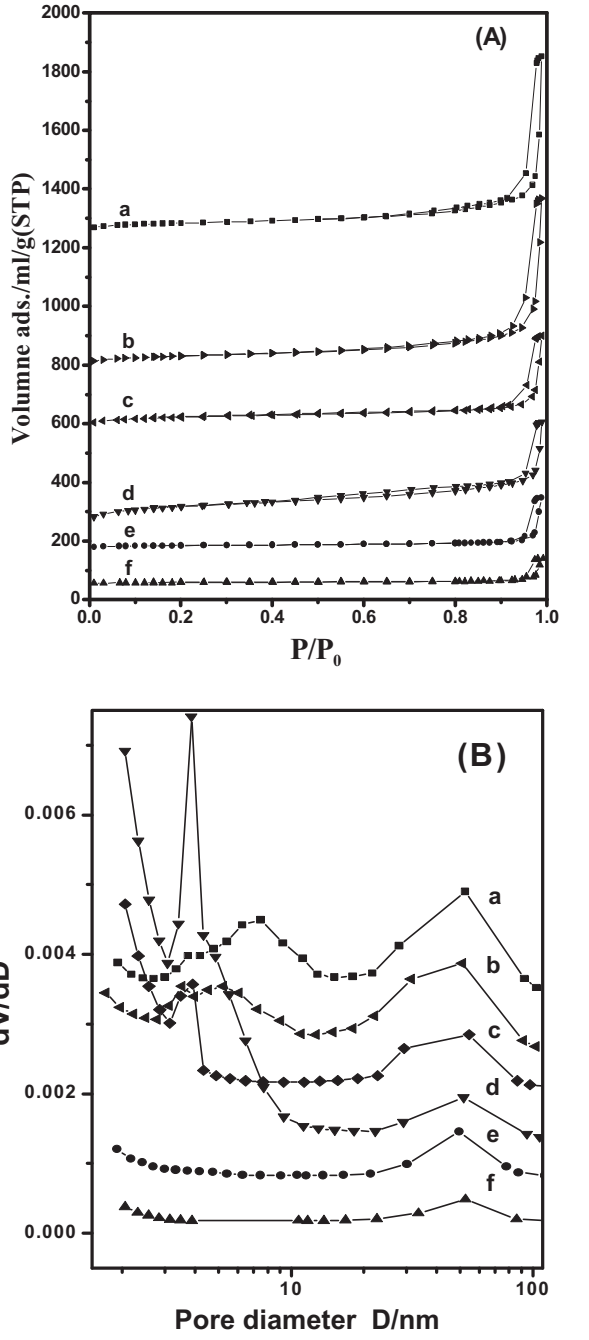

Fig. 4. Nitrogen adsorption/desorption isotherms (A) and BJH pore size distributions (B) for the samples. (a) SiO_2; (b) R-SiO_2; (c) PDVB/R-SiO_2-0.33; (d) PDVB/R-SiO_2-0.5; (e) PDVB/R-SiO_2-1.0; (f) PDVB/R-SiO_2-2.0.

and Applied Chemistry classification) with a sharp capillary condensation step at P/P_0 equal to 0.95, indicating the presence of a mesoporous structure. A hysteresis loop of the H_1 type with a clear step at P/P_0 equal to 0.95 (from the adsorption branch) characterized the pores with cylindrical geometry. The pore size distributions of SiO_2 and R-SiO_2 (3–10 nm and 20–100 nm, respectively) are shown in Fig. 4(B). These distributions indicate the insignificant effect of silane grafting on the porous structure. However, the introduction of PDVB to the pores caused the disappearance of pore distribution ranging from 20 nm to 100 nm and the appearance of new pore sizes. For example, the PDVB/R-SiO_2-0.5 sample exhibited pore size distributions of <2 nm and in the range of 2–5 nm, indicating that PDVB can create new micropores and mesopores. By contrast, the pore distributions of the PDVB/R-SiO_2-1 and PDVB/R-SiO_2-2 samples in the ranges of 4–10 nm and 30–100 nm confirm the pore blockage caused by excess PDVB.

3.1.2. Water contact angle

To identify the surface hydrophobic properties of the samples, the water contact angles of bare SiO_2 and PDVB/R-SiO_2-0.5 were measured (Fig. 5). The water droplet of the silica gel sample was immediately spread on the surface, with a contact angle of zero, indicating high hydrophilicity in the silica gel attributed to its rich surface hydroxyl. When a water droplet was allowed contact with the surface of PDVB/R-SiO_2-0.5, the contact angle measured was 117.3°, suggesting that hydrophobic films on the SiO_2 surface were formed by PDVB coating. Moreover, hydrophobicity may be related to surface roughness, which is consistent with previous findings.

3.2. Dynamic adsorption

Fig. 6 shows the toluene adsorption breakthrough curves of the samples under dry conditions. The curves can be divided into three stages. During the first stage, the toluene was almost completely adsorbed, and its outlet concentration was almost zero. During the second stage, the toluene concentration gradually reached the breakthrough point (the outlet concentration was 5% of the inlet concentration), and the outlet toluene concentration significantly increased with extended adsorption time. The outlet concentration rose in an S-shaped curve to the inlet concentration (i.e., the third stage). In general, the longer the breakthrough time, the higher the dynamic adsorption capacity. Among the samples, PDVB/R-SiO_2-0.5 and PDVB/R-SiO_2-2 exhibited the longest (i.e., nearly 45 min) and the shortest (i.e., only 1 min) breakthrough times, respectively. However, PDVB/R-SiO_2-2 required a longer time to reach adsorption equilibrium. The need for an extended breakthrough time may be attributed to the blockage of the SiO_2 pores by excess PDVB,

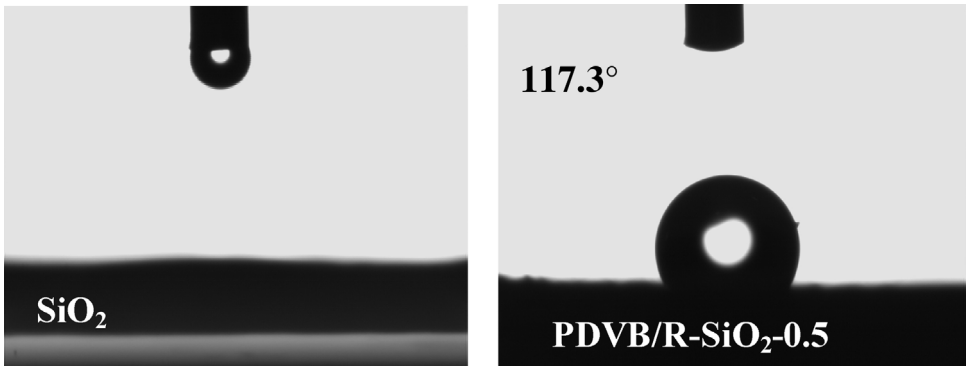

Fig. 5. Photos of a water droplet on a tablet of SiO_2 and PDVB/R-SiO_2-0.5.

thereby increasing the resistance of toluene diffusion from the outer to the inner micropores.

To perform a quantitative comparison of the adsorption capacities between SiO_2 and PDVB/R-SiO_2, the breakthrough curves were fitted using the Yoon and Nelson (Y–N) model. The Y–N equation is expressed as [26]

$$t = \tau + \frac{1}{k'} \ln\left(\frac{C}{C_0 - C}\right)$$

where C_0 and C are inlet and the outlet concentrations of the adsorbate, t is the breakthrough time, K is the constant rate, and τ is the time required for a 50% adsorbate breakthrough.

As shown in Fig. 6 and Table 2, the breakthrough curves of toluene onto samples were fitted well by the Y–N model. For comparison, the adsorption breakthrough times and breakthrough capacities were calculated using the Y–N equation, as shown in Table 2. The saturated adsorption capacity of pure SiO_2 was only 5.2 mg/g. The introduction of PDVB significantly increased toluene adsorption. PDVB/R-SiO_2-0.5 obtained the largest adsorption amount (about 61 mg/g), which was 12 times greater than that of pure SiO_2. The PDVB/R-SiO_2-1.0 and PDVB/R-SiO_2-2.0 samples obtained adsorption amounts lower than PDVB/R-SiO_2-0.5 because of the smaller surface area of the former. Likewise, PDVB/R-SiO_2-2 obtained an adsorption amount of 0.87 mg/m^2, which was 20 times higher than that of pure SiO_2. Therefore, the increase in surface areas was not the primary reason for the increase in adsorption amounts. The microporous and smaller mesoporous structures formed by introducing PDVB was very important for the high adsorption of organic molecules.

To investigate the adsorption properties in a highly humid environment, the dynamic toluene adsorption of SiO_2 and PDVB/R-SiO_2-0.5 in a humid gas stream [40%, 50%, 60%, and 70% relative humidity (RH)] was compared. SiO_2 exhibited high breakthrough peaks after 2 min (i.e., the outlet toluene concentration was higher than the inlet concentration) (Fig. 7). This finding indicates that the toluene molecules were not completely adsorbed on the SiO_2 in a humid environment (50% RH) because the water molecules were strongly adsorbed on the surface by replacing toluene. However, in a different humid environment, the breakthrough curves of PDVB/R-SiO_2-0.5 slightly changed compared with that under dry conditions. This difference may be attributed to the high degree of surface PDVB functionalization. PDVB/R-SiO_2-0.5 is an excellent adsorbent with potential environmental applications owing to its hydrophobicity and appropriate pore diameter.

3.3. Regeneration ability

Thermal regeneration ability is one of the important criteria for excellent VOC adsorption. Fig. 8 shows the breakthrough curves of PDVB/R-SiO_2-0.5, which was regenerated by continuous thermal desorption at 100 °C and adsorption at 40 °C. After at least 10 adsorption/desorption cycles, toluene adsorption remained at approximately 60 mg/g. Absorbed toluene can be completely removed under hot N_2 at 100 °C, and toluene adsorption was only slightly reduced after desorption. Fig. 9 shows the desorption curves of 20 mL/min N_2 gas at 80 °C and 100 °C, the outlet toluene concentration was monitored by GC at an interval of 1 min.

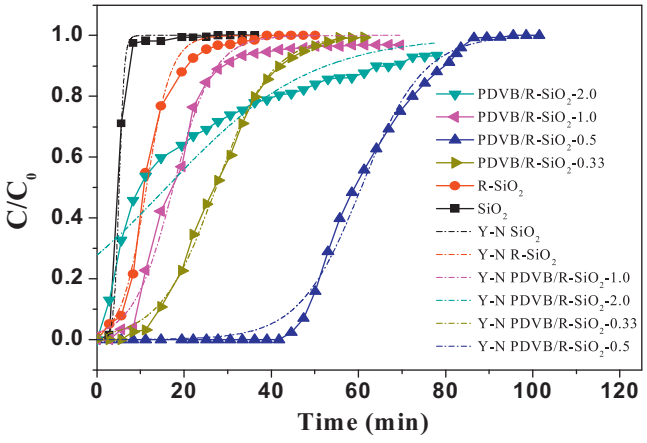

Fig. 6. Experimental and predicted breakthrough curves of toluene on six samples under dry conditions (GHSV: 60,000 mL/(h g), inlet toluene concentration 1000 mg/g).

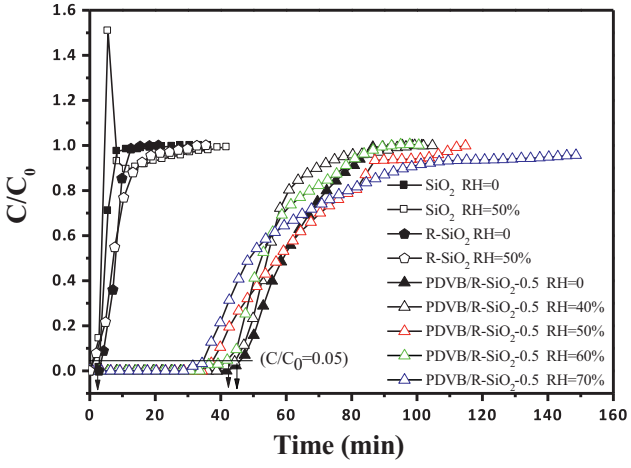

Fig. 7. Comparison of breakthrough curves for toluene adsorbed on SiO_2, R-SiO_2 and PDVB/R-SiO_2-0.5 under dry and humid air conditions (GHSV: 60,000 mL/(h g), inlet toluene concentration 1000 mg/g).

Table 2
Breakthrough characteristics of toluene adsorption onto SiO_2 and PDVB/SiO_2 calculated from Y–N model and experimental data.

Samples	(min)	t_1 (C/C_0 = 0.1) (min)	t_2 (C/C_0 = 0.9) (min)	Saturated adsorption (mg/g)	Break through adsorption (mg/g)	Adsorption per square meter (mg/m^2)
SiO_2	5.084	3.843	6.348	5.216	3.140	0.0438
R-SiO_2	11.360	5.223	17.580	12.25	6.920	0.1216
PDVB/R-SiO_2-0.33	27.316	13.293	41.400	19.36	8.960	0.1448
PDVB/R-SiO_2-0.5	60.667	45.097	76.352	61.01	48.91	0.2475
PDVB/R-SiO_2-1.0	17.501	7.376	27.660	13.90	8.200	0.5034
PDVB/R-SiO_2-2.0	15.920	2.211	52.583	13.64	3.430	0.8715

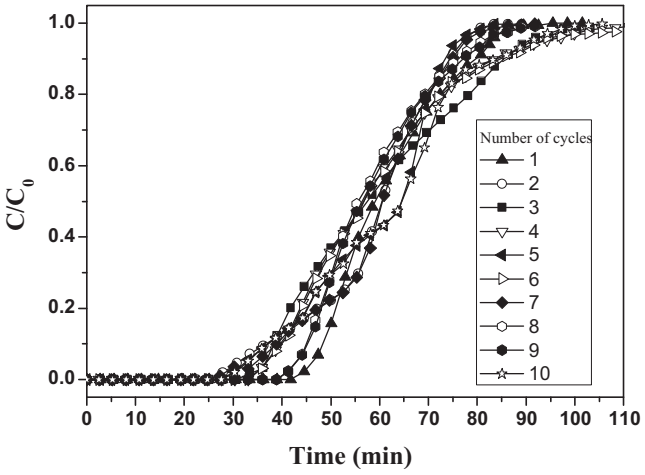

Fig. 8. The breakthrough curves for toluene adsorbed on PDVB/R-SiO_2-0.5 under continuous adsorption–desorption cycle.

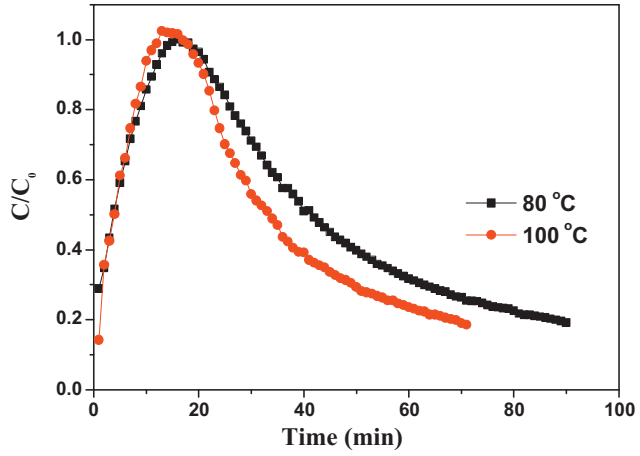

Fig. 9. Desorption curve of N_2 gas at temperatures ranging from 80 °C to 100 °C (toluene concentration C_0, 35 g/m^3; adsorbent amount, 0.5 g; flow volume of N_2, 20 mL/min).

The highest toluene concentration of 35 g/m^3 was observed after 20 min. This concentration is exceeds the saturated vapor concentration of toluene at 0 °C. Toluene adsorbed on PDVB/R-SiO_2-0.5 can be completely desorbed within 60 min. The desorption in the range of 80–100 °C is more energy-effective than that of zeolite Y in the range of 200–250 °C [11]. Therefore, PDVB/R-SiO_2-0.5 exhibits excellent thermal stability and regeneration performance.

4. Conclusions

Introducing DVB to SiO_2 pores and polymerizing under solvothermal conditions yields PDVB/R-SiO_2-0.5, a novel organic–inorganic composite adsorbent material. In contrast to pure SiO_2, PDVB/R-SiO_2-0.5 exhibits a larger surface area, larger pore volume, and smaller pore size distribution. The hydrophilic surface of SiO_2 becomes hydrophobic after PDVB functionalization. The amount of low-concentration toluene adsorbed onto PDVB/R-SiO_2-0.5 is 12 times higher than that adsorbed onto pure SiO_2 and is not affected by high humidity (70% RH). The samples exhibited remarkable regeneration ability. Therefore, PDVB/R-SiO_2 can be an excellent adsorbent in rotary wheels for VOCs removal.

Acknowledgments

We would like to acknowledge the financial support provided by the Natural Science Foundation of China (No. 21107096) and the Natural Science Foundation of Zhejiang Province (No. Y5090202).

References

[1] G.R. Parmar, N.N. Rao, Emerging control technologies for volatile organic compounds, Crit. Rev. Env. Sci. Technol. 39 (2009) 41–78.
[2] M.E. Ramos, P.R. Bonelli, A.L. Cukierman, M.M.L. Ribeiro Carrott, P.J.M. Carrott, Adsorption of volatile organic compounds onto activated carbon cloths derived from a novel regenerated cellulosic precursor, J. Hazard. Mater. 177 (2010) 175–182.
[3] A. Silvestre-Albero, J.M. Ramos-Fernandez, M. Martinez-Escandell, A. Sepulveda-Escribano, J. Silvestre-Albero, F. Rodriguez-Reinoso, High saturation capacity of activated carbons prepared from mesophase pitch in the removal of volatile organic compounds, Carbon 48 (2010) 548–556.
[4] L.Q. Li, Z. Sun, H.L. Li, T.C. Keener, Effects of activated carbon surface properties on the adsorption of volatile organic compounds, J. Air Waste Manage. Assoc. 62 (2012) 1196–1202.
[5] S.W. Nahm, W.G. Shim, Y.K. Park, S.C. Kim, Thermal and chemical regeneration of spent activated carbon and its adsorption property for toluene, Chem. Eng. J. 210 (2012) 500–509.
[6] S.G. Ramalingam, P. Pre, S. Giraudet, L. Le Coq, P. Le Cloirec, O. Baudouin, S. Dechelotte, Different families of volatile organic compounds pollution control by microporous carbons in temperature swing adsorption processes, J. Hazard. Mater. 221 (2012) 242–247.
[7] F. Cosnier, A. Celzard, G. Furdin, D. Begin, J.F. Mareche, O. Barres, Hydrophobisation of active carbon surface and effect on the adsorption of water, Carbon 43 (2005) 2554–2563.
[8] P. Le Cloirec, P. Pre, F. Delage, S. Giraudet, Visualization of the exothermal VOC adsorption in a fixed-bed activated carbon adsorber, Environ. Technol. 33 (2012) 285–290.
[9] D.P. Serrano, G. Calleja, J.A. Botas, F.J. Gutierrez, Characterization of adsorptive and hydrophobic properties of silicalite-1, ZSM-5, TS-1 and beta zeolites by TPD techniques, Sep. Purif. Technol. 54 (2007) 1–9.
[10] D.G. Lee, J.H. Kim, C.H. Lee, Adsorption and thermal regeneration of acetone and toluene vapors in dealuminated Y-zeolite bed, Sep. Purif. Technol. 77 (2011) 312–324.
[11] H.F. Lu, C.H. Zhou, Y. Zhou, H.F. Huang, Y.F. Chen, Adsorption–desorption of toluene in gas phase on dealuminated ultrastable Y zeolites, J. Chem. Eng. Chin. Univ. 26 (2012) 338–343.
[12] C.M. Wang, T.W. Chung, C.M. Huang, H. Wu, Adsorption equilibria of acetate compounds on activated carbon, silica gel, and 13X zeolite, J. Chem. Eng. Data 50 (2005) 811–816.
[13] W.H. Tao, T.C.K. Yang, Y.N. Chang, L.K. Chang, T.W. Chung, Effect of moisture on the adsorption of volatile organic compounds by zeolite 13X, J. Environ. Eng. ASCE 130 (2004) 1210–1216.
[14] M. Guillemot, J. Mijoin, S. Mignard, P. Magnoux, Adsorption of tetrachloroethylene on cationic X and Y zeolites: influence of cation nature and of water vapor, Ind. Eng. Chem. Res. 46 (2007) 4614–4620.
[15] D.P. Serrano, G. Calleja, J.A. Botas, F.J. Gutierrez, Adsorption and hydrophobic properties of mesostructured MCM-41 and SBA-15 materials for volatile organic compound removal, Ind. Eng. Chem. Res. 43 (2004) 7010–7018.

[16] T.M. Wu, G.R. Wu, H.M. Kao, J.L. Wang, Using mesoporous silica MCM-41 for in-line enrichment of atmospheric volatile organic compounds, J. Chromatogr. A 1105 (2006) 168–175.
[17] H.F. Huang, X. Chu, H.F. Lu, B. Zhang, Y. Li, Y.F. Chen, Dynamic adsorption performances and breakthrough curve model of some aromatic VOCs on MCM-41 and SBA-15, J. Chem. Eng. Chin. Univ. 25 (2011) 219–224.
[18] B.J. Dou, Q. Hua, J.J. Li, S.H. Qiao, Z.P. Hao, Adsorption performance of VOCs in ordered mesoporous silicas with different pore structures and surface chemistry, J. Hazard. Mater. 186 (2011) 1615–1624.
[19] Q. Hu, J.J. Li, Z.P. Hao, L.D. Li, S.Z. Qiao, Dynamic adsorption of volatile organic compounds on organofunctionalized SBA-15 materials, Chem. Eng. J. 149 (2009) 281–288.
[20] X.S. Zhao, G.Q. Lu, X. Hub, A novel method for tailoring the pore-opening size of MCM-41 materials, Chem. Commun. (1999) 1391–1392.
[21] K.S. Chang, M.T. Chen, T.W. Chung, Effects of the thickness and particle size of silica gel on the heat and mass transfer performance of a silica gel-coated bed for air-conditioning adsorption systems, Appl. Therm. Eng. 25 (2005) 2330–2340.
[22] G. Zhang, Y.F. Zhang, L. Fang, Theoretical study of simultaneous water and VOCs adsorption and desorption in a silica gel rotor, Indoor Air 18 (2008) 37–43.
[23] K.S. Chang, H.C. Wang, T.W. Chung, Effect of regeneration conditions on the adsorption dehumidification process in packed silica gel beds, Appl. Therm. Eng. 24 (2004) 735–742.
[24] Y.L. Zhang, S. Wei, F.J. Liu, Y.C. Du, S. Liu, Y.Y. Ji, T. Yokoi, T. Tatsumi, F.S. Xiao, Superhydrophobic nanoporous polymers as efficient adsorbents for organic compounds, Nano Today 4 (2009) 135–142.
[25] P. Liu, C. Long, Q. Li, H. Qian, A. Li, Q. Zhang, Adsorption of trichloroethylene and benzene vapors onto hypercrosslinked polymeric resin, J. Hazard. Mater. 166 (2009) 46–51.
[26] C. Long, W.H. Yu, A.M. Li, Adsorption of n-hexane vapor by macroporous and hypercrosslinked polymeric resins: equilibrium and breakthrough analysis, Chem. Eng. J. 221 (2013) 105–110.